Peer-reviewed version available at *Atmosphere* **2017**, *8*, 114; doi:10.3390/atmos8070114

*Article*

# Monthly and Diurnal Variation of the Concentrations of Aerosol Surface Area in Fukuoka, Japan, Measured by Diffusion Charging Method

**Miho Kiriya [1], Tomoaki Okuda [1,*], Hana Yamazaki [1], Kazuki Hatoya [1], Naoki Kaneyasu [2], Itsushi Uno [3], Chiharu Nishita [4], Keiichiro Hara [4], Masahiko Hayashi [4], Koji Funato [5], Kozo Inoue [5], Shigekazu Yamamoto [6], Ayako Yoshino [7] and Akinori Takami [7]**

[1] Faculty of Science and Technology, Keio University, 3-14-1 Hiyoshi, Kohoku-ku, Yokohama 223-8522, Japan; miear.k.117@gmail.com (M.K.); hanayamazaki@z5.keio.jp (H.Y.); k.hatoya.ec@gmail.com (K.H.)
[2] Atmospheric Environment Research Group, National Institute of Advanced Industrial Science and Technology, Tsukuba, Ibaraki 305-8569, Japan; kane.n@aist.go.jp
[3] Research Institute for Applied Mechanics, Kyushu University, Fukuoka, Fukuoka 816-8580, Japan; uno@riam.kyushu-u.ac.jp
[4] Faculty of Science, Fukuoka University, Fukuoka 814-0180, Japan; cnishita@fukuoka-u.ac.jp (C.N.); harakei@fukuoka-u.ac.jp (K.H.); mhayashi@fukuoka-u.ac.jp (M.H.)
[5] Tokyo Dylec Corp., Shinjuku, Tokyo 160-0014, Japan; k-funato@tokyo-dylec.co.jp (K.F.); inoue@tokyo-dylec.co.jp (K.I.)
[6] Fukuoka Institute of Health and Environmental Sciences, Dazaifu, Fukuoka 818-0135, Japan; yamamoto-s8309@pref.fukuoka.lg.jp
[7] Center for Regional Environmental Research, National Institute for Environmental Studies, Tsukuba, Ibaraki 305-8506, Japan; yoshino.ayako@nies.go.jp (A.Y.); takamia@nies.go.jp (A.T.)
* Correspondence: okuda@applc.keio.ac.jp; Tel./Fax: +81-45-566-1578

**Abstract:** Observation of the ambient aerosol surface area concentrations is important to understand the aerosol toxicity because an increased surface area may be able to act as an enhanced reaction interface for certain reactions between aerosol particles and biological cells, as well as an augmented carrier surface for co-pollutants. In this study, the concentration of aerosol surface area was measured from April 2015 to March 2016 in Fukuoka, Japan. We investigated the monthly and diurnal variations in the correlations between the aerosol surface area and black carbon (BC) and sulfate concentrations. Throughout the year, aerosol surface area concentration was strongly correlated with the concentrations of BC, which has relatively large surface area since BC particles are usually submicron agglomerates consisting of much smaller (tens of nanometers) sized primary soot particles. The slopes of the regression between the aerosol surface area and BC concentrations was highest in August and September 2015. This appears to have been the results of an increase in the proportion of the airmass that originated on the main islands of Japan. This may enhance the introduction of the BC from the main islands of Japan that is relatively fresh (or "uncoated"), thereby maintaining its larger surface area.

**Keywords:** Asian monsoon; black carbon; long-range transport; land and sea breeze; sulfate; surface area; surface coating of particles

## 1. Introduction

Many studies investigating the adverse effects of exposure to ambient aerosols on human health have been conducted. This is based on the globally acknowledged possibility that these aerosols are hazardous to humans [1-3]. In particular, ultrafine particles with a diameter less than 100 nm (nanoparticles) are considered to be more harmful than larger particles [4-7]. Surface area is considered as an appropriate indicator in compared to mass for evaluating pulmonary inflammatory

Peer-reviewed version available at Atmosphere 2017, 8, 114; doi:10.3390/atmos8070114

responses for rats or mice caused by exposure to manufactured nanomaterials, such as $TiO_2$, fullerenes, and carbon nanotubes [8-11]. The surface area measurement is also important to understand the aerosol toxicity because an increased surface area may be able to act as an enhanced reaction interface for certain reactions between aerosol particles and biological cells, as well as an augmented carrier surface for co-pollutants [12,13].

The most popular method to measure the particle specific surface area is the Brunauer-Emmett-Teller (BET) method [14]. The toxicity led by exposure to manufactured materials related to the specific surface area has been discussed on the basis of the BET specific surface area values [8-10]. However, it is challenging to experimentally measure the actual surface area of atmospheric aerosol particles due to limitations on the quantity of aerosols that can be collected using ordinary sampling methods [15-17].

Other practical and continuous techniques are required to measure the concentrations of ambient aerosol surface area. A nanoparticle surface area monitor (NSAM) using the diffusion charging method has been developed for continuous measurement for the concentration of particle surface area [17-22]. Particles introduced in the NSAM are forced to be charged with positive ions emitted by corona discharger in a mixing chamber, and then the particle charges are measured by an electrometer installed in the downstream. The particle surface area is calculated based on the assumption that it is ideally proportional to the particle charge [18]. The actual NSAM output is the lung-deposited surface area (LDSA) concentration of particles that can be converted to the concentration of ambient aerosol surface area [17,22-27]. These previous reports presented that the concentration of aerosol surface area is strongly correlated with the concentrations of black carbon (BC) and polycyclic aromatic hydrocarbons in particulate phase. These facts are reasonable since BC (or BC-like) particles are usually submicron agglomerates consisting of much smaller (tens of nanometers) sized primary soot particles [26, 28].

However, the ways in which chemical species other than BC and meteorological conditions contribute to the variation in the concentrations of ambient aerosol surface area is not well understood. Particularly, sulfate aerosols may occasionally have a significant effect on aerosol surface area concentration [22]. In this study, we measured the concentration of aerosol surface area together with BC and sulfate, as well as meteorological data for one year at Fukuoka, Japan, and investigated the effect of the aerosol chemical compositions and meteorological conditions on the aerosol surface area. This study is a follow-up experiment of Okuda *et al.* (2016) [22] in order to perform a year-round investigation of aerosol surface area and some related parameters.

## 2. Experiments

### *2.1. Observation Site and Period*

The monitoring site for the aerosol surface area, BC, and particle number concentrations was the fourth floor of a building of the Fukuoka Institute for Atmospheric Environment and Health (33.55°N, 130.36°E) at Fukuoka University, Japan [22, 29-31]. Another monitoring site for the sulfate concentration was the Fukuoka Institute of Health and Environmental Science (33.51˚N, 130.48˚E). These two sites are ~15 km distant from each other. Fukuoka city is one of the largest cities in northern Kyushu district, which faces the Asian continent (Figure 1). Generally, sulfate concentrations in this area (northern Kyushu district) are governed by a long-range transport, and exhibit very similar variation over 100 km scale of location [29]. For example, sulfate in Fukue and Fukuoka showed very similar concentration level and variation even though these two sites are approximately 200 km distant from each other [29]. Therefore, the 15 km of distance between these two observational sites can be ignored when we focus on the sulfate concentration in this area. The area and population of Fukuoka city were approximately 340 $km^2$ and 1.5 million, respectively. Aerosols observed in Fukuoka originate on the continent and in the local area. This site is therefore well situated for an examination of differences in aerosol surface area and chemical composition between aerosol sources. $PM_{2.5}$ concentrations over this site are generally affected by the long-range transport process from the Asian continent [29, 32]. Observation period was from 1 April 2015 to 31 March 2016.

Peer-reviewed version available at *Atmosphere* **2017**, *8*, 114; doi:10.3390/atmos8070114

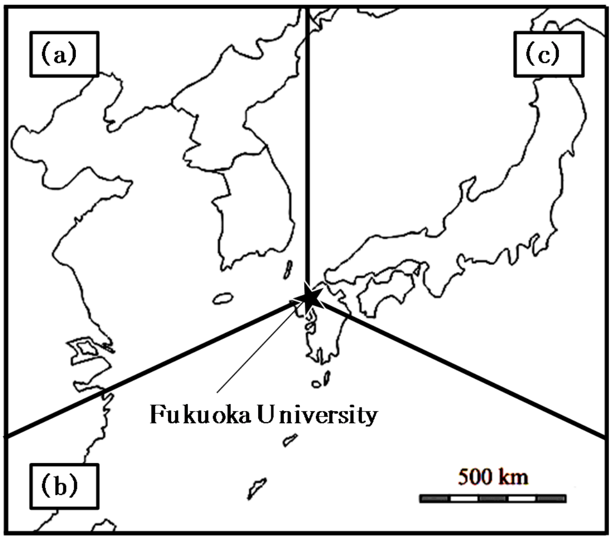

**Figure 1.** Map of East Asia showing each sector classified by airmass backward trajectories from the monitoring site (Fukuoka University, Japan): (a) Asian continent, (b) southern part of Kyushu, and (c) main islands of Japan.

### *2.2. Aerosol Surface Area*

The surface area concentration was measured using an NSAM (Model 3550, TSI Inc., MN, USA). The flow rate of the NSAM was 2.5 L min$^{-1}$, and the time resolution was set to 10 min. The NSAM has a cyclone with a 50% cut-off of 1 μm at the inlet; thus, the quantity the NSAM measures is actually the surface area concentration of $PM_{1.0}$. The procedure for the conversion from LDSA (the actual NSAM reading) to aerosol surface area has already been described elsewhere [17,22], but is briefly summarized here. The calibration constant is determined with passing monodisperse aerosols simultaneously through the scanning mobility particle sizer (SMPS) and the NSAM by the manufacturer (TSI. Inc.). Specifically, the total surface area of the 80-nm NaCl particles determined by the SMPS is multiplied by the lung deposition efficiency of 80-nm particles, which is determined using the lung deposition curve for a reference worker reported by the International Commission on Radiological Protection [33]. In this study, we measured tracheobronchial-deposited surface area values using the NSAM, and then converted them into aerosol surface area by dividing them by the ICRP deposition efficiency of 80-nm particles. In order to check the validity of the calibration constant, we measured the total surface area of polydisperse $SiO_2$ particles (sicastar, micromod Partikeltechnologie GmbH, Rostock, Germany) using SMPS and NSAM simultaneously. The surface area concentrations were calculated using particle diameters of the spherical particle. The results are shown in Figure 2. The surface area measured by NSAM matched very well with that measured by SMPS. Therefore, we applied this calibration constant to the field measurement results obtained in this study.

### *2.3. Black Carbon, Aerosol Number and Mass, Sulfate Ion Concentration, and Wind Direction and Speed*

The mass concentration of BC in $PM_{2.5}$ was measured using an aethalometer (AE-16U, Magee Scientific Corp., CA, USA) [32]. A Sharp-Cut Cyclone SCC1.829 (BGI Inc., NJ, USA) was used as the $PM_{2.5}$ inlet. The BC concentration measured using an aethalometer based on the rate of absorption of incident light (880 nm) by BC shows reasonable agreement with elemental carbon (EC) measured using the thermal-optical method [34,35]. The flow rate of the aethalometer was 5.0 L min$^{-1}$, and the time resolution was set to 15 min.

Peer-reviewed version available at *Atmosphere* **2017**, *8*, 114; doi:10.3390/atmos8070114

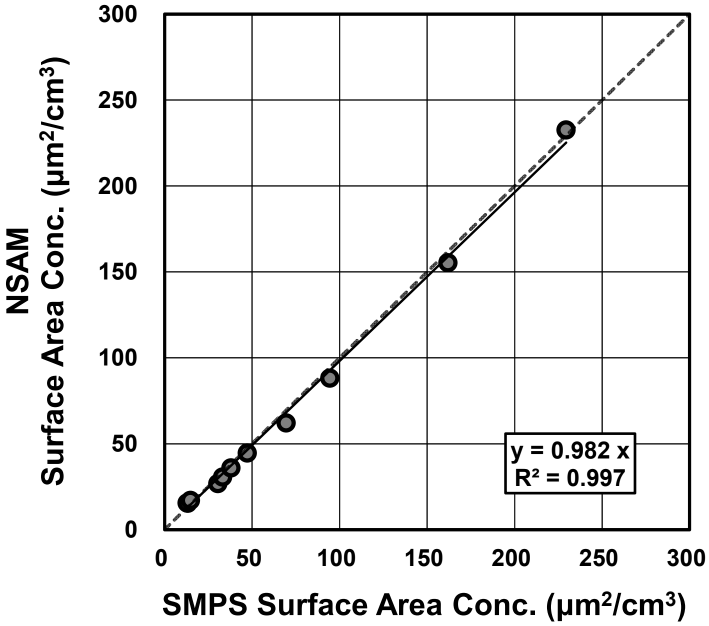

**Figure 2.** Map of East Asia showing each sector classified by airmass backward trajectories from the monitoring site (Fukuoka University, Japan): (a) Asian continent, (b) southern part of Kyushu, and (c) main islands of Japan.

Sulfate concentrations were measured and analyzed using a continuous dichotomous aerosol chemical speciation analyzer (ACSA-12, Kimoto Electric Co., Ltd., Japan). The ACSA-12 determines the sulfate ion concentration using the $BaSO_4$-based turbidimetric method after the addition of $BaCl_2$ dissolved in polyvinyl pyrrolidone solution, and the results correspond closely with the values determined using the denuder-filter method [36].

The aerosol number concentrations and particle size distributions (optical equivalent diameter: > 0.3, > 0.5, > 1.0, > 2.0, > 3.0, and > 5.0 µm) were measured using an optical particle counter (OPC, TD100; Sigma Tech., Yokohama, Japan), which was installed on the rooftop of the building in Fukuoka University, and operated in ambient conditions without using a heating drier. The size discriminator of the OPC was calibrated using polystyrene latex spheres with a refractive index of 1.59-0i. The OPC data were corrected for coincidence loss. The flow rate of the OPC was 1.0 L min$^{-1}$, and the time resolution was set to 1 min.

$PM_{2.5}$ mass concentration, wind direction, and wind speed data were obtained from websites operated by national and local governmental offices [37,38]

The time resolution varied according to the instrument or the sources of the downloaded data. As a result, we used 1-h average values for all further analyses in this study. All times are expressed according to the local time zone (JST: UTC + 9h).

### *2.4. Airmass Backward Trajectory Analysis*

Airmass backward trajectories were calculated for each day of the measurement campaign using the NOAA HYSPLIT model [39,40]. The trajectories were calculated based on the following conditions: start latitude and longitude: 33.55°N, 130.36°E; start altitude: 1500 m above sea level; and calculation time: 72h (three days). The trajectories were calculated every 3 hours (0:00 to 21:00 of local time) and were allocated to one of three sectors ((a) Asian continent, (b) southern Kyushu, and (c) main islands of Japan, see Fig. 1) if the trajectory positions for every 6-h interval were within the sector at least 36h (50% of the time) and if the trajectory positions were within other sectors less than 24 h (33% of the time).

## 3. Results and Discussion

### *3.1. Diurnal Variations*

Table 1 shows the mean values of the concentrations of aerosol surface area, $PM_{2.5}$ mass, BC, sulfate, and particle number measured in this study. The mean concentrations of surface area and other variables measured in this study were not so different from those presented in several previous papers [17,22-24,29].

**Table 1.** Mean and standard deviation of each variable measured in this study in Fukuoka, Japan (April 2015 to March 2016, 1-h average value).

| | | **Mean** | **SD** | ***n*** |
|---|---|---|---|---|
| Surface Area | $\mu m^2\ cm^{-3}$ | 127 | 62 | 8032 |
| $PM_{2.5}$ mass | $\mu g\ m^{-3}$ | 17.3 | 10.7 | 8064 |
| BC | $ng\ m^{-3}$ | 579 | 430 | 7698 |
| $SO_4^{2-}$ | $\mu g\ m^{-3}$ | 4.94 | 3.17 | 7413 |
| Particle Number (>0.3 μm) | # $cm^{-3}$ | 419 | 469 | 7281 |

The diurnal variations of each variable were analyzed to investigate the effect of diurnal human activity on the concentration of aerosol surface area (Figure 3). The concentrations of aerosol surface area and BC in the morning (8:00-10:00) were significantly higher than at other times (*t*-test, $p < 0.01$). Apparently, concentrated automotive traffic near the monitoring site resulted in the morning peak of aerosol surface area and BC [22-24,26,29].

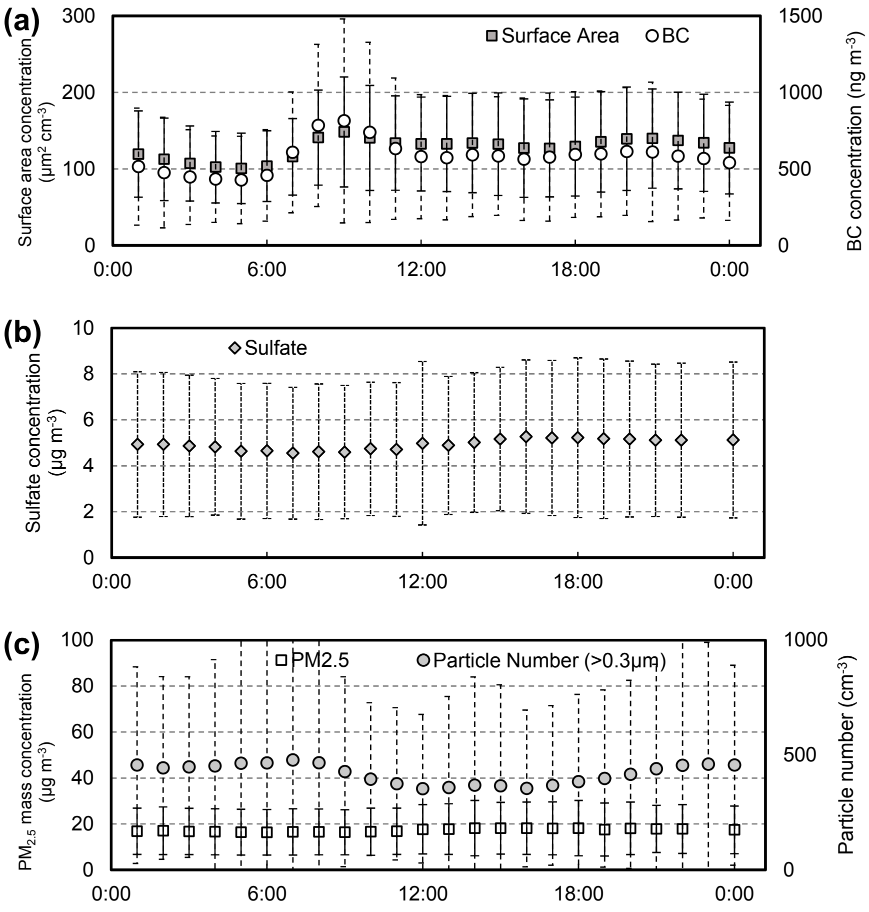

**Figure 3.** Diurnal variation in (a) aerosol surface area and BC concentrations; (b) sulfate concentrations; (c) $PM_{2.5}$ mass concentration and particle number (> 0.3 μm), measured from April 2015 to March 2016 in Fukuoka, Japan.

Peer-reviewed version available at *Atmosphere* **2017**, *8*, 114; doi:10.3390/atmos8070114

The other variables did not exhibit morning peaks. This finding is supported by a previous study that suggested that the elemental carbon in Fukuoka City originated mainly from local emission sources rather than from long-range transport [29]. Of all the variables, BC was consistently the most strongly correlated with aerosol surface area over the observation site. This fact means that we should pay much attention to BC when considering the aerosol surface area as a metric of adverse health effects caused by exposure to aerosols.

A detailed investigation of the diurnal variation of the aerosol surface area and BC concentrations are shown in Figure 4. The aerosol surface area and BC concentrations exhibited a clear daily morning peak in winter (October to March). On the other hand, the morning peak of BC concentration was unclear in summer (April to September). Besides, the aerosol surface area concentration in the afternoon was much higher than that in the morning in summer. Correlation plots of the aerosol surface area vs. BC concentrations are shown in Figure 5. The correlation between the aerosol surface area and BC concentrations was much stronger in winter than summer. The high-surface area-low-BC type plots were found frequently in summer, but not much in winter. Apparently, there are some reasons that the aerosol surface area become high other than the BC concentration in the afternoon in summer. The seasonal variations are discussed in the following sections.

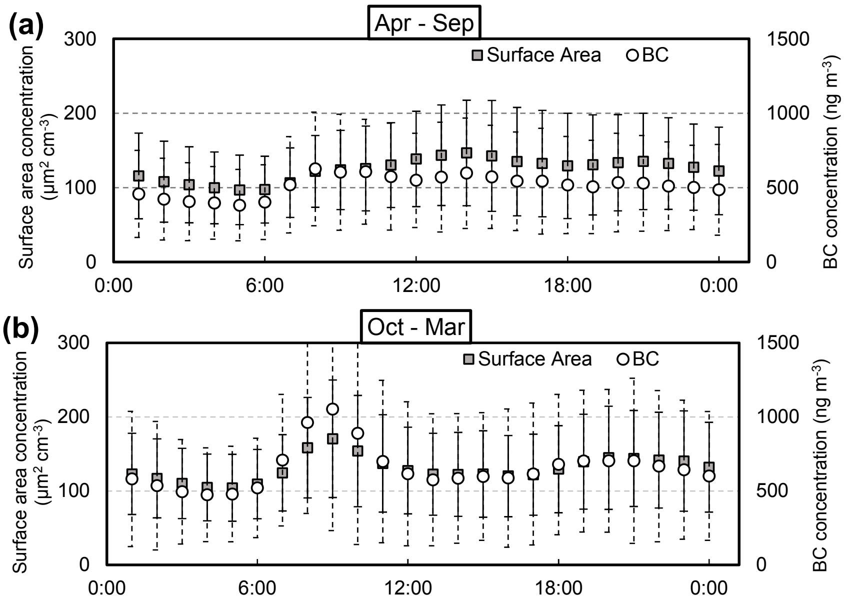

**Figure 4.** Diurnal variation in the aerosol surface area and BC concentrations in Fukuoka, Japan, measured from (a) April to September 2015, and (b) October 2015 to March 2016.

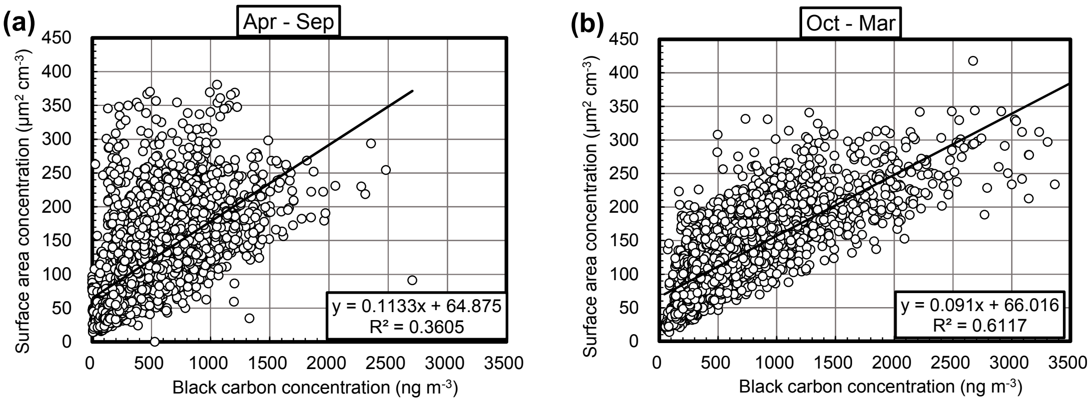

**Figure 5.** Correlation plots of the aerosol surface area vs. BC concentrations in Fukuoka, Japan, measured from (a) April to September 2015, and (b) October 2015 to March 2016.

**Table 2.** Linear regressions between black carbon concentration or sulfate concentration and the aerosol surface area concentration for each month from continuous measurements conducted from April 2015 to March 2016.

**Surface Area *vs* BC**

| Year | Month | Slope (µm² cm⁻³) / (ng m⁻³) | Intercept µm² cm⁻³ | Coefficient of determination | *n* |
|---|---|---|---|---|---|
| 2015 | Apr | 0.12 | 40 | 0.45 | 489 |
| | May | 0.093 | 81 | 0.41 | 659 |
| | Jun | 0.11 | 73 | 0.23 | 696 |
| | Jul | 0.10 | 100 | 0.23 | 625 |
| | Aug | 0.15 | 44 | 0.42 | 511 |
| | Sep | 0.17 | 39 | 0.62 | 678 |
| | Oct | 0.088 | 77 | 0.54 | 623 |
| | Nov | 0.10 | 51 | 0.59 | 546 |
| | Dec | 0.089 | 55 | 0.76 | 374 |
| 2016 | Jan | 0.079 | 64 | 0.71 | 535 |
| | Feb | 0.12 | 57 | 0.66 | 713 |
| | Mar | 0.13 | 46 | 0.64 | 632 |

**Surface Area *vs* $SO_4^{2-}$**

| Year | Month | Slope (µm² cm⁻³) / (ng m⁻³) | Intercept µm² cm⁻³ | Coefficient of determination | *n* |
|---|---|---|---|---|---|
| 2015 | Apr | 0.0072 | 72 | 0.21 | 508 |
| | May | 0.0068 | 99 | 0.10 | 651 |
| | Jun | 0.0084 | 70 | 0.33 | 676 |
| | Jul | 0.0034 | 112 | 0.030 | 570 |
| | Aug | 0.0056 | 87 | 0.15 | 460 |
| | Sep | 0.014 | 65 | 0.22 | 641 |
| | Oct | 0.0073 | 110 | 0.15 | 642 |
| | Nov | 0.017 | 80 | 0.12 | 427 |
| | Dec | 0.013 | 77 | 0.18 | 335 |
| 2016 | Jan | 0.013 | 62 | 0.22 | 653 |
| | Feb | 0.0070 | 98 | 0.081 | 630 |
| | Mar | 0.0063 | 78 | 0.12 | 655 |

### *3.2. Monthly Correlations between Aerosol Surface Area and BC Concentrations*

The correlation between the aerosol surface area and BC concentrations was analyzed on a monthly basis to investigate this relationship in more detail. Table 2 shows the slopes and intercepts of regression lines, the coefficients of determination, and the number of data in the correlation between aerosol surface area and BC or sulfate concentrations for each month through the year. The correlation between the aerosol surface area and BC concentrations was strong for all months except June and July ($R^2 = 0.41$-$0.76$), for which the coefficients of determination was low ($R^2 = 0.23$). In these cases it is possible that the sulfate concentration caused the aerosol surface area concentrations to increase substantially [22]. The coefficient of determination in the correlation between the aerosol surface area and sulfate concentrations was higher in June ($R^2 = 0.33$) than in other months ($R^2 = 0.030$-$0.22$; Table 2). The correlations between the aerosol surface area and sulfate concentrations were showed in Fig. 6, and that in June (Fig. 6(a)) actually shows that the high concentrations of sulfate increased aerosol surface area concentrations. These events did not appear in other months. For June, the number of data points for which the hourly sulfate concentration was ≥ 15 µg m⁻³ and the aerosol surface area concentration was ≥ 150 µm² cm⁻³ was extremely large (Fig. 7). That is, high sulfate concentrations increased aerosol surface area concentrations, which resulted in a weakening of the correlation between the aerosol surface area and BC concentrations. According to a previous study,

Peer-reviewed version available at Atmosphere 2017, 8, 114; doi:10.3390/atmos8070114

high-sulfate-high-surface area events were possibly caused by volcanic $SO_2$ [22]. However, in this study $SO_2$ concentrations did not increase in June at Fukuoka. The reason for the high sulfate concentrations in June 2015 in Fukuoka was therefore not volcanic gas. Furthermore, the coefficient of determination in the correlation between the aerosol surface area and sulfate concentrations was not high in July ($R^2$ = 0.030; Fig. 6b); on the contrary, it was the lowest of the year (Table 2). We therefore surmise that other chemical compounds, such as organic carbon, may have contributed to the July aerosol surface area concentration in Fukuoka.

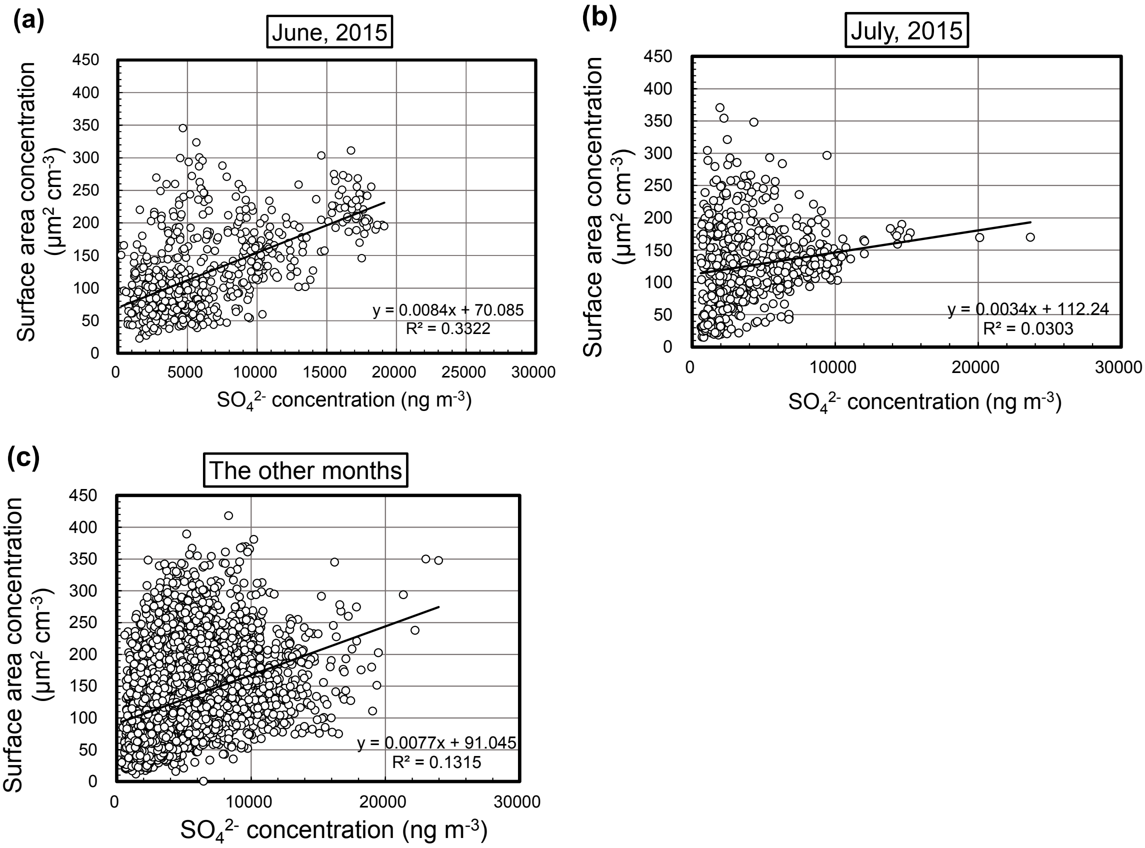

**Figure 6.** Comparison between the aerosol surface area and sulfate concentrations recorded in continuous measurements, for (a) June, (b) July, and (c) the other months of the study.

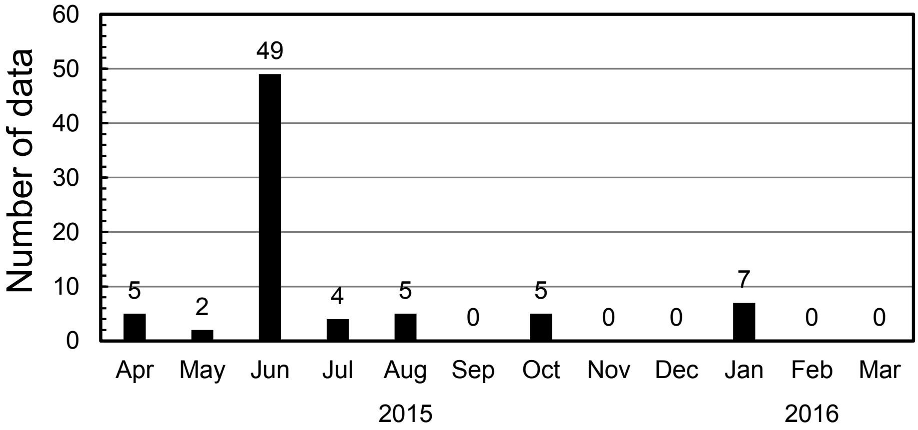

**Figure 7.** The monthly number of data points for which the sulfate concentration was ≥ 15 μg m⁻³ and the surface area concentration was ≥ 150 μm² cm⁻³ in Fukuoka.

Peer-reviewed version available at Atmosphere 2017, 8, 114; doi:10.3390/atmos8070114

The slopes of the regression between the aerosol surface area and BC concentrations, and thus the ratio of the former to the latter, in August and September was larger than in the other months (Table 2). This appears to have been the result of different airmass sources in summer from the rest of the year. The proportion of the airmass originating in continental Asia was smaller in July, August, and September than in the rest of the year, and the proportion coming from the main islands of Japan was greater in August and September (Fig. 8). In Japan, meteorological conditions are generally dominated by the Asian monsoon. As a result, the prevailing wind direction was easterly in August and September 2015 in Fukuoka city. From our results, therefore, we can conclude that the BC from the Asian continent did not have a large surface area but have a high mass concentration, whereas, the mass concentrations of BC transported by easterly wind was low, but those BC had larger surface area. A possible explanation for this is that some chemical compounds were adsorbed to (or "coated") the surface of the BC during its long-range transport [41-43], therby reducing its surface area. Conversely, BC from the main islands of Japan was relatively fresh (or "uncoated"), thereby maintaining its larger surface area. This caused the slopes of the regression between the aerosol surface area and BC concentrations for August and September to increase, but did not reduce the coefficient of determination.

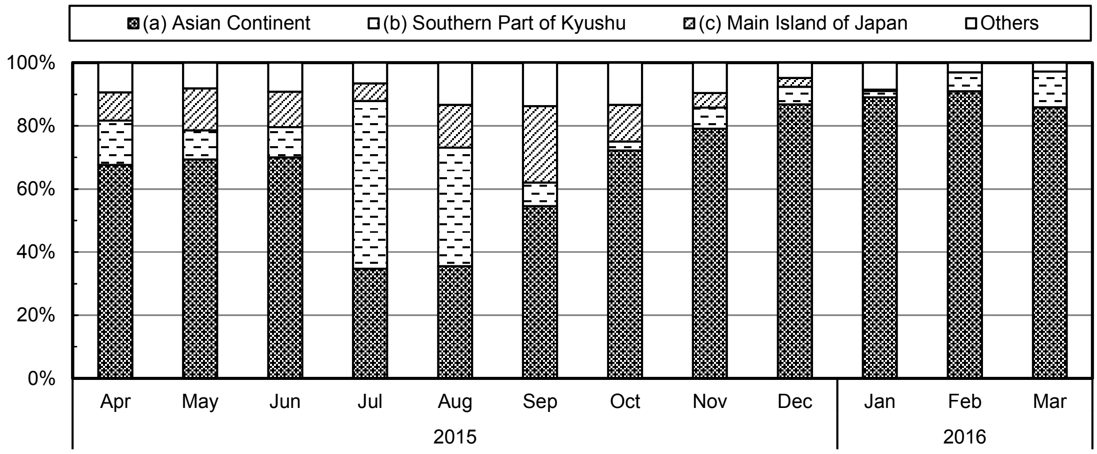

**Figure 8.** Monthly airmass backward trajectory analysis, starting at Fukuoka, from April 2015 to March 2016. The sector classification is shown in Figure 1.

### *3.3. Effect of Land and Sea Breeze on the Correlation between Aerosol Surface Area and Black Carbon Concentrations*

As we have seen, the correlation between the aerosol surface area and BC concentrations varied from month to month as a result of sulfate input or coating of BC surfaces. In this section we discuss how this correlation changed with time of day. We divided the day into four segments: (a) night (0:00-6:00), (b) morning (6:00-12:00), (c) afternoon (12:00-18:00), and (d) evening (18:00-24:00). Table 3 shows the correlation between the aerosol surface area and BC concentrations in the four time segments. The coefficients of determination for the afternoon ($R^2$ = 0.07-0.71) in particular was lower than that for the other times (night: 0.41-0.87, morning: 0.09-0.84, and evening: 0.29-0.81). This diurnal variation can be related to wind direction and speed. Fukuoka lies on the coast of the Sea of Japan, and is thus often subject to the land and sea breeze. Fig. 9 shows a diurnal variation in wind speed and wind direction in Fukuoka from April 2015 to March 2016. In Fukuoka, the direction of sea breezes is northerly (0°) and that of land breezes is southerly (180°). We generally recorded a sea breeze during the afternoon (12:00 to 18:00), which was strongest from 13:00 to 16:00 (~ 4 m $s^{-1}$), and a gentler land breeze (~2 m $s^{-1}$) at night and the early morning. This may have caused that BC concentrations decrease in the afternoon due to the inflow of a clean airmass via the sea breeze. The nocturnal reversal of the wind direction back to the land breeze would then prevents any further decrease in BC concentrations. Fig. 10 shows the BC concentrations corresponding to the wind direction and wind speed. These plots clearly shows that stronger northerly winds make the BC concentration low. In addition, sulfate concentrations were higher in the afternoon (12:00-18:00) than at other times (*t*-test, $p<0.01$; Fig. 3b). Generally, sulfate is formed by oxidation of $SO_2$, and this reaction is promoted by solar radiation (i.e. during the daytime). The additional sulfate particles formed would thus contribute to the aerosol surface area concentration. This explains the lower coefficients of determination between the aerosol surface area and BC concentrations in the afternoon and the reversal of this pattern in the evening (Table 3).

**Table 3.** Linear regressions between the aerosol surface area and black carbon (BC) concentrations in the four time segments: (**a**) night (0:00-6:00), (**b**) morning (6:00-12:00), (**c**) afternoon (12:00-18:00), and (**d**) evening (18:00-24:00). The measurements were conducted from April 2015 to March 2016.

| | | **(a) night (0:00-6:00)** | | | | **(b) morning (6:00-12:00)** | | | |
|---|---|---|---|---|---|---|---|---|---|
| **Year** | **Month** | **Slope ($\mu m^2$ $cm^{-3}$) / (ng $m^{-3}$)** | **Intercept $\mu m^2$ $cm^{-3}$** | **Coefficient of determination** | ***n*** | **Slope ($\mu m^2$ $cm^{-3}$) / (ng $m^{-3}$)** | **Intercept $\mu m^2$ $cm^{-3}$** | **Coefficient of determination** | ***n*** |
| 2015 | Apr | 0.12 | 30 | 0.87 | 119 | 0.068 | 70 | 0.17 | 112 |
| | May | 0.12 | 62 | 0.47 | 172 | 0.070 | 83 | 0.42 | 160 |
| | Jun | 0.17 | 52 | 0.41 | 174 | 0.095 | 72 | 0.27 | 173 |
| | Jul | 0.15 | 36 | 0.63 | 163 | 0.051 | 102 | 0.09 | 149 |
| | Aug | 0.20 | 24 | 0.70 | 136 | 0.094 | 68 | 0.25 | 124 |
| | Sep | 0.19 | 28 | 0.70 | 164 | 0.12 | 55 | 0.48 | 160 |
| | Oct | 0.10 | 69 | 0.60 | 161 | 0.085 | 74 | 0.70 | 153 |
| | Nov | 0.13 | 40 | 0.63 | 138 | 0.088 | 51 | 0.74 | 135 |
| | Dec | 0.091 | 45 | 0.78 | 92 | 0.085 | 47 | 0.84 | 89 |
| 2016 | Jan | 0.080 | 51 | 0.68 | 132 | 0.083 | 65 | 0.76 | 132 |
| | Feb | 0.11 | 59 | 0.64 | 174 | 0.12 | 60 | 0.74 | 169 |
| | Mar | 0.13 | 47 | 0.50 | 156 | 0.11 | 57 | 0.61 | 156 |

| | | **(c) afternoon (12:00-18:00)** | | | | **(d) evening (18:00-24:00)** | | | |
|---|---|---|---|---|---|---|---|---|---|
| **Year** | **Month** | **Slope ($\mu m^2$ $cm^{-3}$) / (ng $m^{-3}$)** | **Intercept $\mu m^2$ $cm^{-3}$** | **Coefficient of determination** | ***n*** | **Slope ($\mu m^2$ $cm^{-3}$) / (ng $m^{-3}$)** | **Intercept $\mu m^2$ $cm^{-3}$** | **Coefficient of determination** | ***n*** |
| 2015 | Apr | 0.12 | 50 | 0.31 | 128 | 0.16 | 21 | 0.68 | 130 |
| | May | 0.084 | 95 | 0.30 | 160 | 0.12 | 74 | 0.62 | 167 |
| | Jun | 0.072 | 99 | 0.13 | 178 | 0.15 | 78 | 0.29 | 171 |
| | Jul | 0.060 | 119 | 0.07 | 155 | 0.14 | 53 | 0.45 | 157 |
| | Aug | 0.15 | 48 | 0.34 | 122 | 0.22 | 13 | 0.59 | 123 |
| | Sep | 0.18 | 34 | 0.62 | 174 | 0.21 | 27 | 0.71 | 168 |
| | Oct | 0.087 | 79 | 0.32 | 151 | 0.091 | 82 | 0.53 | 158 |
| | Nov | 0.096 | 61 | 0.36 | 140 | 0.13 | 43 | 0.72 | 133 |
| | Dec | 0.089 | 56 | 0.71 | 95 | 0.10 | 64 | 0.81 | 98 |
| 2016 | Jan | 0.063 | 73 | 0.63 | 133 | 0.083 | 73 | 0.71 | 138 |
| | Feb | 0.099 | 61 | 0.49 | 172 | 0.15 | 49 | 0.69 | 174 |
| | Mar | 0.12 | 46 | 0.56 | 159 | 0.17 | 29 | 0.81 | 161 |

## 4. Conclusions

We measured the aerosol surface area, black carbon (BC), and sulfate concentrations for one year in Fukuoka, Japan, and investigated the monthly and diurnal variations in the correlation between the aerosol surface area and BC concentrations. Throughout the year, the aerosol surface area concentration was strongly correlated with BC concentration. In June 2015, the coefficient of determination for this correlation was lower than in other months, as a result of high sulfate concentrations. In August and September 2015, the slopes of the regression between the aerosol surface area and BC concentrations was highest. This appears to have been the results of an increase in the proportion of the airmass that originated on the main islands of Japan. This may enhance the introduction of the BC from the main islands of Japan that is relatively fresh (or "uncoated"), thereby maintaining its larger surface area. In addition, the correlation between the aerosol surface area and BC concentrations was weakest in the afternoon because certain secondary formed aerosols increase. This may be also because Fukuoka is generally dominated by the land and sea breeze, and BC concentrations decrease under those conditions due to the afternoon inflow of a clean airmass.

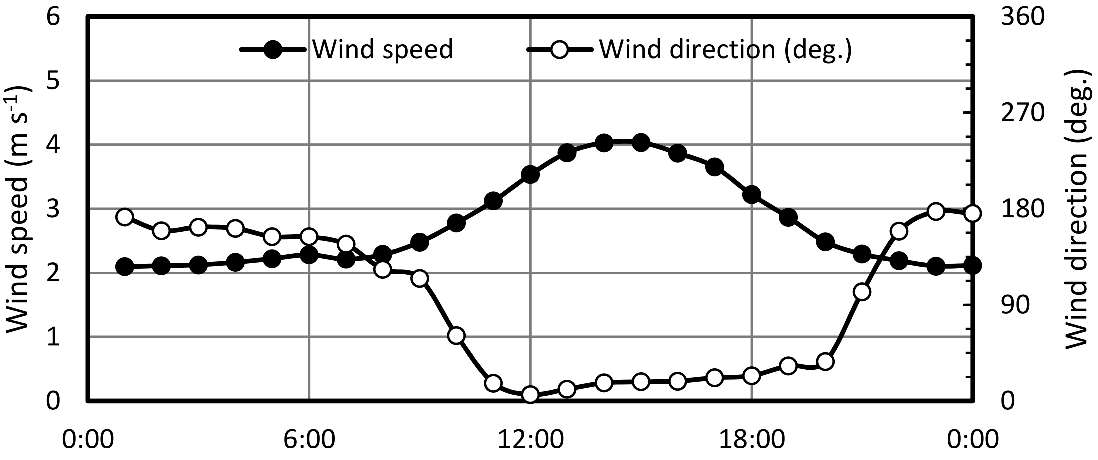

**Figure 9.** Diurnal variation in wind speed and wind direction in Fukuoka, measured from April 2015 to March 2016. Wind directions as follows: 0°: Northerly, 90°; Easterly, 180°; Southerly; and 270°: Westerly.

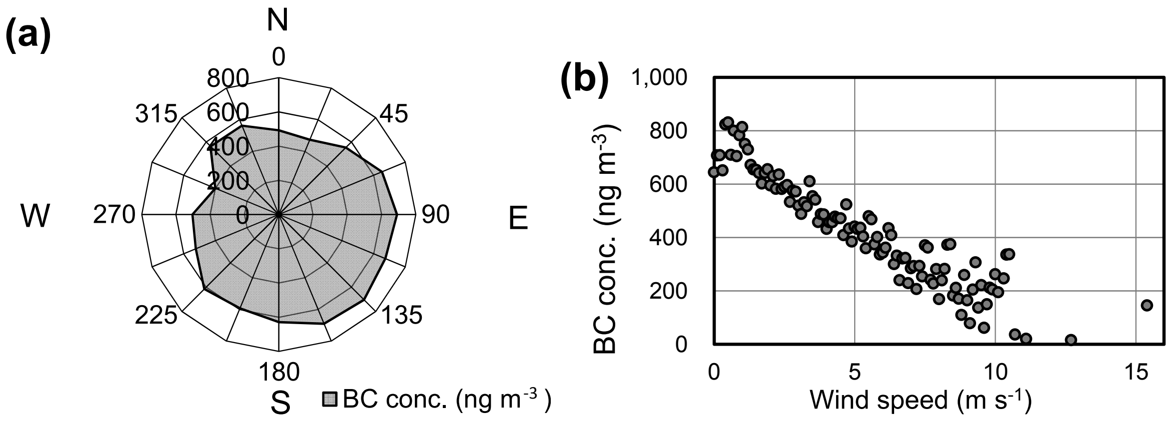

**Figure 10.** BC concentrations corresponding to (a) the wind direction, and (b) the wind speed, in Fukuoka, measured from April 2015 to March 2016.

**Acknowledgments:** This study was partly supported by JSPS/MEXT KAKENHI Grant Numbers 26340010 and JP25220101, Ministry of Environment, Environment Research and Technology Development Fund, Japan (Grant Nos. 5-1452 and 5-1651), Grant for Environmental Research Projects from The Sumitomo Foundation, Steel Foundation for Environmental Protection Technology, and Keio Gijuku Academic Development Funds.

**Author Contributions:** T.O. conceived and designed the experiments, and wrote the paper; M.K. analyzed the data and wrote the draft of paper, H.Y. analyzed the data; K.H. (Keio Univ.) , K.F. and K.I. installed and operated the NSAM, N.K. performed the BC measurements; I.U. and S.Y. installed and operated the ACSA, A.Y., A.T., C.N., K.H. (Fukuoka Univ.) and M.H. administrated the entire experiments. All authors contributed to revising the manuscript.

**Conflicts of Interest:** The authors declare no conflict of interest. The founding sponsors had no role in the design of the study; in the collection, analyses, or interpretation of data; in the writing of the manuscript, and in the decision to publish the results.

## References

1. Dockery, D.W.; Pope, C.A., III; Xu, X.; Spengler, J.D.; Ware, J.H.; Fay, M.E.; Ferris, B.G., Jr.; Speizer, F.E. An association between air pollution and mortality in six U.S. cities. *N. Engl. J. Med.* **1993**, *329*, 1753–1759.
2. Pope, C.A., III; Thun, M.J.; Namboodiri, M.M.; Dockery, D.W.; Evans, J.S.; Speizer, F.E.; Heath, C.W., Jr. Particulate air pollution as a predictor of mortality in a prospective study of U.S. adults. *Am. J. Respir. Crit. Care Med.* **1995**, *151*, 669–674.
3. International Agency for Research on Cancer. *Air Pollution and Cancer*; IARC Scientific Publication: Lyon, France, 2013; No. 161.
4. Ferin, J.; Oberdörster, G.; Penney, D.P. Pulmonary retention of ultrafine and fine particles in rats. *Am. J. Respir. Cell Mol. Biol.* **1992**, *6*, 535–542.
5. Oberdörster, G.; Gelein, R.M.; Ferin, J.; Weiss, B. Association of particulate air pollution and acute mortality: Involvement of ultrafine particles? *Inhal. Toxicol.* **1995**, *7*, 111–124.
6. Donaldson, K.; Li, X.Y.; MacNee, W. Ultrafine (nanometre) particle mediated lung injury. *J. Aerosol Sci.* **1998**, *29*, 553–560.
7. The National Institute for Occupational Safety and Health (NIOSH). *The National Institute for Occupational Safety and Health (NIOSH): Approaches to Safe Nanotechnology*; DHHS (NIOSH) Publication No. 2009-125; The National Institute for Occupational Safety and Health (NIOSH): Washington, DC, USA, 2009.
8. Oberdörster, G.; Finkelstein, J.N.; Johnston, C.; Gelein, R.; Cox, C.; Baggs, R.; Elder, A.C.P. Acute pulmonary effects of ultrafine particles in rats and mice. *Res. Rep. Health Eff. Inst.* **2000**, *96*, 5–74.
9. Oberdörster, G.; Oberdörster, E.; Oberdörster, J. Nanotoxicology: An emerging discipline evolving from studies of ultrafine particles. *Environ. Health Perspect.* **2005**, *113*, 823–839.
10. Nakanishi, J. Risk Assessment of Manufactured Nanomaterials: Carbon Nanotubes (CNT). Final Report Issued on August 12, 2011, Executive Summary; NEDO project "Research and Development of Nanoparticle Characterization Methods." (P06041); New Energy and Industrial Technology Development Organization: Kawasaki, Japan, 2011.
11. Schmid, O.; Stoeger, T. Surface area is the biologically most effective dose metric for acute nanoparticle toxicity in the lung. *J. Aerosol Sci.* **2016**, *99*, 133-143.
12. Oberdörster, G. Pulmonary effects of inhaled ultrafine particles. *Int. Arch. Occup. Environ. Health* **2001**, *74*, 1–8.
13. Giechaskiel, B.; Alföldy, B.; Drossinos, Y. A metric for health effects studies of diesel exhaust particles. *J. Aerosol Sci.* **2009**, *40*, 639–651.
14. Brunauer, S.; Emmett, P.H.; Teller, E. Adsorption of gases in multimolecular layers. *J. Am. Chem. Soc.* **1938**, *60*, 309–319.
15. Okuda, T. Measurement of the specific surface area and particle size distribution of atmospheric aerosol reference materials. *Atmos. Environ.* **2013**, *75*, 1–5.
16. Okuda, T.; Isobe, R.; Nagai, Y.; Okahisa, S.; Funato, K.; Inoue, K. Development of a high-volume $PM_{2.5}$ particle sampler using impactor and cyclone techniques. *Aerosol Air Qual. Res.* **2015**, *15*, 759–767.
17. Hatoya, K.; Okuda, T.; Funato, K.; Inoue, K. On-line measurement of the surface area concentration of aerosols in Yokohama, Japan, using the diffusion charging method. *Asian J. Atmos. Environ.* **2016**, *10, 1-12.*
18. Jung, H.; Kittelson, D.B. Characterization of aerosol surface instruments in transition regime. *Aerosol Sci. Technol.* **2005**, *39*, 902–911.
19. Fissan, H.; Neumann, S.; Trampe, A.; Pui, D.Y.H.; Shin, W.G. Rationale and principle of an instrument measuring lung deposited nanoparticle surface area. *J. Nanopart. Res.* **2007**, *9*, 53–59.
20. Shin, W.G.; Pui, D.Y.H.; Fissan, H.; Neumann, S.; Trampe, A. Calibration and numerical simulation of Nanoparticle Surface Area Monitor (TSI Model 3550 NSAM). *J. Nanopart. Res.* **2007**, *9*, 61–69.
21. Heitbrink, W.A.; Evans, D.E.; Ku, B.K.; Maynard, A.D.; Slavin, T.J.; Peters, T.M. Relationships among particle number, surface area, and respirable mass concentrations in automotive engine manufacturing. *J. Occup. Environ. Hyg.* **2009**, *6*, 19–31.

22. Okuda, T.; Yamazaki, H.; Hatoya, K.; Kaneyasu, N.; Yoshino, A.; Takami, A.; Funato, K.; Inoue, K.; Nishita, C.; Hara, K.; Hayashi, M. Factors Controlling the Variation of Aerosol Surface Area Concentrations Measured by a Diffusion Charger in Fukuoka, Japan. *Atmosphere* **2016**, *7*, 33.
23. Velasco, E.; Siegmann, P.; Siegmann, H.C. Exploratory study of particle-bound polycyclic aromatic hydrocarbons in different environments of Mexico City. *Atmos. Environ.* **2004**, *38*, 4957–4968.
24. Ntziachristos, L.; Polidori, A.; Phuleria, H.; Geller, M.D.; Sioutas, C. Application of a diffusion charger for the measurement of particle surface concentration in different environments. *Aerosol Sci. Technol.* **2007**, *41*, 571–580.
25. Asbach, C.; Fissan, H.; Stahlmecke, B.; Kuhlbusch, T.A.J.; Pui, D.Y.H. Conceptual limitations and extensions of lung-deposited Nanoparticle Surface Area Monitor (NSAM). *J. Nanopart. Res.* **2009**, *11*, 101–109.
26. Albuquerque, P.C.; Gomes, J.F.; Bordado, J.C. Assessment of exposure to airborne ultrafine particles in the urban environment of Lisbon, Portugal. *J. Air Waste Manag. Assoc.* **2012**, *62*, 373–380.
27. Gomes, J.F.P.; Albuquerque, P.C.S.; Esteves, H.M.D.S.; Carvalho, P.A. Notice on a methodology for characterizing emissions of ultrafine particles/nanoparticles in microenvironments. *Energy Emiss. Cont. Technol.* **2013**, *1*, 15–27, doi:10.2147/EECT.S48148.
28. China, S.; Salvadori, N.; Mazzoleni, C. Effect of traffic and driving characteristics on morphology of atmospheric soot particles at freeway on-ramps. *Environ. Sci. Technol.* **2014**, *48*, 3128–3135.
29. Kaneyasu, N.; Yamamoto, S.; Sato, K.; Takami, A.; Hayashi, M.; Hara, K.; Kawamoto, K.; Okuda, T.; Hatakeyama, S. Impact of long-range transport of aerosols on the $PM_{2.5}$ composition at a major metropolitan area in the northern Kyushu area of Japan. *Atmos. Environ.* **2014**, *97*, 416–425.
30. Takami, A.; Miyoshi, T.; Irei, S.; Yoshino, A.; Sato, K.; Shimizu, A.; Hayashi, M.; Hara, K.; Kaneyasu, N.; Hatakeyama, S. Analysis of organic aerosol in Fukuoka, Japan using a PMF method. *Aerosol Air Qual. Res.* **2016**, *16*, 314–322.
31. Yoshino, A.; Takami, A.; Sato, K.; Shimizu, A.; Kaneyasu, N.; Hatakeyama, S.; Hara, K.; Hayashi, M. Influence of Trans-Boundary Air Pollution on the Urban Atmosphere in Fukuoka, Japan, *Atmosphere* **2016**, *7*, 51.
32. Kaneyasu, N.; Takami, A.; Sato, K.; Hatakeyama, S.; Hara, S.; Kawamoto, K.; Yamamoto, S. Year-round behavior of $PM_{2.5}$ in a remote island and urban site in the northern Kyushu area, Japan. *J. Jpn. Soc. Atmos. Environ.* **2011**, *46*, 111–118. (In Japanese)
33. International Commission on Radiological Protection (ICRP). Human respiratory tract model for radiological protection. *Ann. ICRP* **1994**, *24*, 1–482.
34. Venkatachari, P.; Zhou, L.; Hopke, P.K.; Schwab, J.J.; Demerjian, K.L.; Weimer, S.; Hogrefe, O.; Felton, D.; Rattigan, O. An intercomparison of measurement methods for carbonaceous aerosol in the ambient air in New York City. *Aerosol Sci. Technol.* **2006**, *40*, 788–795.
35. Ng, I.P.; Ma, H.; Kittelson, D.B.; Miller, A.L. *Comparing Measurements of Carbon in Diesel Exhaust Aerosols Using the Aethalometer, NIOSH Method 5040, and SMPS*; SAE Technical Paper Series 2007-01-0334; University of Minnesota: Minneapolis, MN, USA, 2007.
36. Osada, K.; Kamiguchi, Y.; Yamamoto, S.; Kuwahara, S.; Pan, X.; Hara, Y.; Uno, I. Comparison of ionic concentrations on size-segregated atmospheric aerosol particles based on a denuder-filter method and a Continuous Dichotomous Aerosol Chemical Speciation Analyzer (ACSA-12), *Earozoru Kenkyu* **2016**, *31*, 203-209. (In Japanese)
37. Fukuoka Prefecture Website. Available online: http://www.fihes.pref.fukuoka.jp/taiki-new/Nipo/OyWbNpKm0151.htm (accessed on 6 May 2017).
38. Japan Meteorological Agency Website. Available online: http://www.data.jma.go.jp/obd/stats/etrn/index.php (accessed on 6 May 2017).
39. Stein, A.F.; Draxler, R.R.; Rolph, G.D.; Stunder, B.J.B.; Cohen, M.D.; Ngan, F. NOAA's HYSPLIT atmospheric transport and dispersion modeling system, *Bull. Amer. Meteor. Soc.* **2015**, *96*, 2059-2077.
40. Rolph, G.D. *Real-time Environmental Applications and Display sYstem (READY) Website*; NOAA Air Resources Laboratory: Silver Spring, MD, USA, 2017.
41. China, S.; Scarnato, B.; Owen, R.C.; Zhang, B.; Ampadu, M.T.; Kumar, S.; Dzepina, K.; Dziobak, M.P.; Fialho, P.; Perlinger, J.A.; Hueber, J.; Helmig, D.; Mazzoleni, L.R.; Mazzoleni, C. Morphology and mixing state of aged soot particles at a remote marine free troposphere site: Implications for optical properties. *Geophys. Res. Lett.* **2015**, *42*, 1243–1250.

Peer-reviewed version available at *Atmosphere* **2017**, *8*, 114; doi:10.3390/atmos8070114

42. Shiraiwa, M.; Kondo, Y.; Moteki, N.; Takegawa, N.; Sahu, L.K.; Takami, A.; Hatakeyama, S.; Yonemura, S.; Blake, D.R. Radiative impact of mixing state of black carbon aerosol in Asian outflow. *J. Geophys. Res.* **2008**, *113*, D24210.
43. Takami, A.; Mayama, N.; Sakamoto, T.; Ohishi, K.; Irei, S.; Yoshino, A.; Hatakeyama, S.; Murano, K.; Sadanaga, Y.; Bandow, H.; Misawa, K.; Fujii, M. Structural analysis of aerosol particles by microscopic observation using a time-of-flight secondary ion mass spectrometer, *J. Geophys. Res. Atmos.* **2013**, *118*, 6726–6737.